

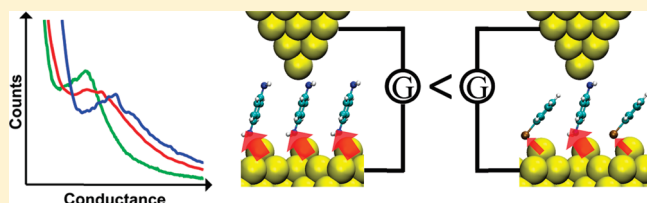
Environmental Control of Single-Molecule Junction Transport

V. Fatemi,^{†,§} M. Kamenetska,[†] J. B. Neaton,^{*,‡} and L. Venkataraman^{*,†}[†]Department of Applied Physics and Applied Mathematics, Columbia University, New York, New York 10027, United States[‡]Molecular Foundry, Lawrence Berkeley National Laboratory, Berkeley, California 94720, United States

§ Supporting Information

ABSTRACT: The conductance of individual 1,4-benzenediamine (BDA)–Au molecular junctions is measured in different solvent environments using a scanning tunneling microscope based point-contact technique. Solvents are found to increase the conductance of these molecular junctions by as much as 50%. Using first principles calculations, we explain this increase by showing that a shift in the Au contact work function is induced by solvents binding to undercoordinated Au sites around the junction. Increasing the Au contact work function reduces the separation between the Au Fermi energy and the highest occupied molecular orbital of BDA in the junction, increasing the measured conductance. We demonstrate that the solvent-induced shift in conductance depends on the affinity of the solvent to Au binding sites and also on the induced dipole (relative to BDA) upon adsorption. Via this mechanism, molecular junction level alignment and transport properties can be statistically altered by solvent molecule binding to the contact surface.

KEYWORDS: Metal–organic interface, single-molecule conductance, tunnel coupling, solvent effects, density functional theory, ρ -phenylenediamine



The past decade has seen rapid progress toward the understanding and control of molecular-scale transport phenomena^{1–3} While advances have been made in understanding how intrinsic factors, such as intramolecular configuration and binding geometry, affect the molecular junction conductance,^{4–9} uncertainties regarding extrinsic factors remain. In particular, the role of the liquid or solvent environment, which are often necessary in nanoscale electronic transport measurements, is generally not addressed in experiments and often neglected in theoretical calculations.¹⁰ Understanding the impact of solvents on molecular junction conductance will serve to elucidate ways in which nanoscale device properties may be manipulated through control of their environment.

Here, we report and explain the modification of the conductance of a single molecule junction through the solvent environment. We use 1,4-benzenediamine (BDA)–Au molecular junctions as a test bed, as past measurements and calculations have shown that its conductance is well-defined and reproducible and originates with specific metal–molecule contact geometries.^{4,11,12} BDA junction conductances (G_{BDA}) are measured with a scanning tunneling microscope-based break junction technique¹³ in 13 different ambient-solvated environments. We observe that G_{BDA} varies by more than 50%, depending on the solvent. First-principles density functional theory (DFT) calculations indicate that like BDA, select solvent molecules can also bind to undercoordinated Au atoms on the electrodes. The smaller surface dipoles induced by a solvent molecule (relative to BDA) lead to a larger Au contact work function and shift the BDA HOMO toward the Au Fermi level (E_{F}), resulting in a larger conductance. We show that solvent-induced shift in conductance depends on (1) the affinity of the solvent to Au binding sites, which affects surface coverage, and (2) the induced dipole upon

adsorption. With this mechanism, molecular junction level alignment and transport properties can be controllably altered by solvent molecule binding to the contact surface.

Single molecule junctions are created by repeatedly forming and breaking an Au point-contact in a 1 mM solution of the BDA under a 25 mV bias with a pulling rate of 15 nm/s in a home-built scanning tunneling microscope.¹⁴ Conductance (current/voltage) is measured as a function of tip/sample displacement to generate conductance traces (Figure 1B inset). The process of breaking an Au point-contact in a solution of BDA creates numerous undercoordinated Au atoms on each electrode, where the amine-terminal groups can bind to form single-molecule junctions. Conductance traces show plateaus at multiples of the quantum of conductance, $G_0 = 2e^2/h$, as the tip–surface contact area is reduced, followed by either a tunneling background or an additional conductance plateau due to the formation of a BDA junction.

Normalized histograms of the conductance traces in three representative solvents—chlorobenzene (ClPh), bromobenzene (BrPh), and iodobenzene (IPh)—are shown in Figure 1A (measurements for all solvents are shown in Figure S1 in the Supporting Information). We see that the peak positions, which give us the most probable junction conductance, are highly solvent-dependent; the Br- and I-based solvents shift the conductance peak to larger values relative to ClPh. Furthermore, experiments in BrPh, which evaporates after about 5000 traces, show a peak at $8.2 \times 10^{-3} G_0$ when solvent is present and $\sim 7 \times 10^{-3} G_0$ immediately after solvent evaporation. The lower conductance value compares well with the

Received: January 27, 2011

Revised: April 10, 2011

Published: April 18, 2011

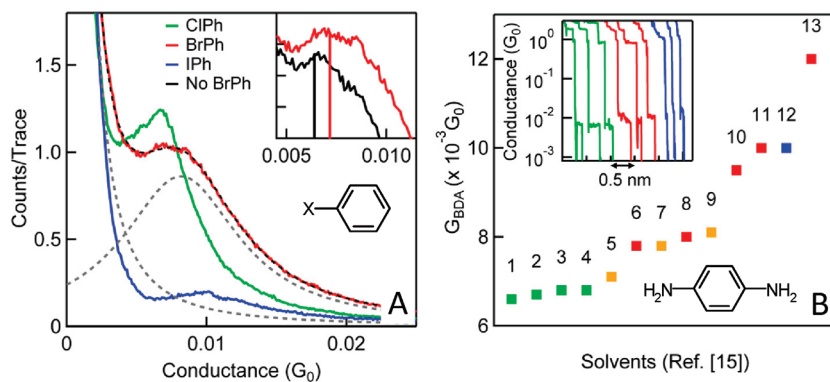


Figure 1. (A) Conductance histograms of BDA junctions in three representative solvents constructed with over 6000 measurements (CIPh in green, BrPh in red, and IPh in blue). Dashed black line show the fit to the BrPh histogram, which is a sum of a power law and Lorentzian. The power law and Lorentzian components are also shown by gray dashed lines. Upper inset: Conductance histogram when BrPh is present (red) and after evaporation (black). Bin size is $10^{-4} G_0$. Lower inset: Chemical structure of solvents (X is either Cl, Br, or I). (B) Conductance of BDA, determined from a Lorentzian fit to histogram data, measured in 13 different solvents.¹⁵ Color indicates the type of functional group on the solvent molecule: green is Cl, red is Br, blue is I, orange is other. The size of the marker represents the error bar in the peak positions. Inset: Example traces in each of the three representative solvents.

conductance peak values for BDA in chlorinated solvents (see inset of Figure 1A). This shift is reversible; the conductance increases once again when additional BrPh solvent is added to the same tip/sample pair. Measurements with solvent alone do not yield plateaus in conductance traces or peaks in conductance histograms as shown in Figure S2 in the Supporting Information. As we will show later, we believe the common lower conductance value occurs when all available binding sites on the tip and substrate are covered by BDA rather than a mixture of solvent and BDA. Figure 1A also shows that the area under the peak and peak width depends on the solvent, as is most clearly visible in measurements in IPh (see also Figures S3 and Table 1 in the Supporting Information). This is due to a significant change in both the junction plateau length, which is shorter in IPh than in CIPh and BrPh (see Figure 1B inset, and Figure S2 in the Supporting Information), and the probability of junction formation, which is lower by about 50% for measurements in IPh when compared with the other two solvents. Additionally, for measurements in IPh, there are successive sets of 1000 traces that do not show a clear conductance peak (not included in Figure 1A), indicating that molecular junctions are not always formed. Finally, we see that this solvent-dependent effect is not specific to BDA. Measurements with 4,4'-diaminostilbene show the same trends in conductance, with almost a factor of 2 increase in conductance when comparing measurements in a chlorinated solvent to that in IPh (Figure S4, Supporting Information).

Conductance peak positions for BDA junctions determined in all 13 solvents investigated¹⁵ are shown in Figure 1B. The choice of solvents was restricted to commercially available high-purity and high boiling point solvents with varying solvent parameters such as molecular dipole moment, permittivity, and chemical substituents such as halogens on the hydrocarbon backbone. These conductance trends shown in Figure 1B do not correlate with either the solvents' intrinsic molecular dipole moments or with their bulk dielectric constants (Figure S5, Supporting Information). For example, BDA junctions measured in CIPh (solvent 1), 1,2,4-trichlorobenzene (solvent 2), and 1,2-dichlorobenzene (solvent 3) are observed to be very similar even though these solvents have very different molecular dipole moments. This suggests that long-ranged solvent–BDA electrostatic interactions are an unlikely mechanism for the observed conductance

modulation. However, the BDA junction conductance is known to arise from nonresonant tunneling through the BDA HOMO,¹¹ with a magnitude that depends on the alignment of the HOMO relative to E_F . Any changes in the induced dipole upon molecular adsorption to binding sites on the tip or surface will affect this alignment. We thus hypothesize that the nature and coverage of such adsorbates (both solvent and BDA molecules) can influence conductance by altering the induced surface dipole and vacuum potential, shifting the BDA HOMO relative to the Au Fermi energy. Since G_{BDA} is low in chlorine containing solvents, higher in solvents with bromine groups, and nearly highest in the solvent with an iodine group, we focus the remainder of our study on three representative halogen containing solvents—CIPh (#1), BrPh (#8), and IPh (#12) which are structurally identical—and explore their binding affinity and effect on level alignment with first-principles density functional theory (DFT) calculations.

We use DFT to compute the work function, Kohn–Sham HOMO energies, and binding energies of BDA and solvent molecules to undercoordinated binding sites on an Au(111) surface. All calculations are performed with the VASP code¹⁶ using the generalized gradient approximation (GGA)¹⁷ and the projector augmented wave (PAW) formalism.¹⁸ A Γ -centered $2 \times 2 \times 1$ k-point mesh and a 500 eV plane-wave cutoff energy result in good convergence of all total-energy calculations. All geometries are optimized until Hellmann–Feynman forces on atoms are less than 0.03 eV/Å. Our supercell consists of a five-layer 4×4 Au(111) slab geometry with two Au adatom binding sites and two molecules. Previous studies have shown that variations in contact geometry do not significantly change the BDA–Au junction electronic structure.¹¹ Because E_{HOMO} tracks the BDA conductance, we forego a full transmission calculation with a second electrode in what follows. Dipole corrections^{19,20} are used to reduce unphysical electrostatic interactions between the slab and its periodic images. Approximately 30 Å of vacuum is included between the Au surface and the top of the unit cell so that the electrostatic potential reaches a constant value in the vacuum region.

We first consider a single BDA molecule bound to one of the two adatom binding sites in our 4×4 supercell, and compute

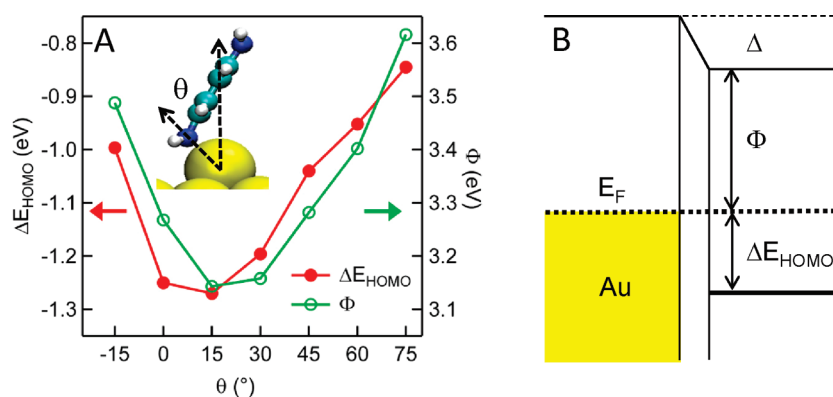


Figure 2. (A) ΔE_{HOMO} and Φ as a function of θ , the angle of the N–Au bond relative to the surface normal. (B) An illustration of how the band structure changes with the addition of a surface dipole induced vacuum level shift Δ .

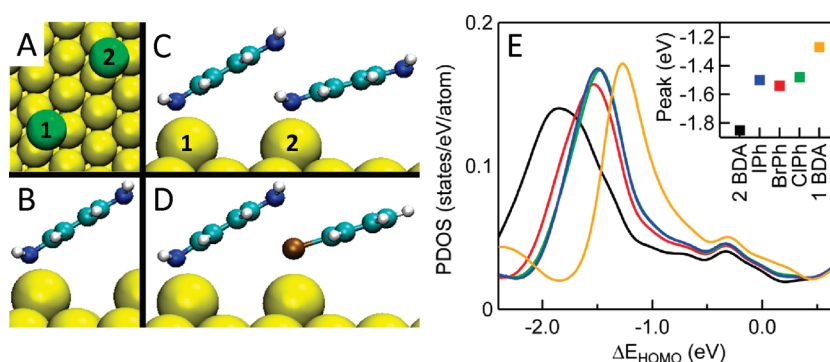


Figure 3. (A) A top-down view of the gold surface showing adatoms 1 and 2 in green. (B, C, D) Side-view snapshots of geometries with a single BDA, two BDA, and BDA and BrPh. θ is 15° for the BDA bonded to adatom 1. (E) Partial density of states of the N atom on the BDA bound to adatom 1 when adatom 2 has no molecule (yellow), a solvent molecule at 0° angle (red, green, blue for BrPh, ClPh, and IPh), and a second BDA (black) at a 0° angle. Inset: ΔE_{HOMO} for each trace.

level alignment and work function for different orientations of the Au–N bond relative to the surface, as illustrated in Figure 2A. We compute the work function Φ for seven different geometries defined by the angle of the N–Au bond relative to the surface normal, θ , and determine the position of the Kohn–Sham HOMO relative to E_F (ΔE_{HOMO}) from the peak in the N-projected partial density of states (PDOS).²¹ We note here that although orbital energies are significantly underestimated by Kohn–Sham DFT within the GGA,^{22–24} the work functions Φ and adsorbate-induced changes in level alignment due to induced dipole effects can be captured accurately.^{25,26} In what follows, we elucidate trends in ΔE_{HOMO} and Φ with θ and surface coverage.

In Figure 2A, we see that ΔE_{HOMO} correlates closely with Φ for the range of geometries investigated. This can be understood by considering the induced surface dipole at the N–Au bond. This donor–acceptor bond involves some charge transfer from molecule to surface which results in a significant charge reorganization within the unit cell inducing a surface dipole. This surface dipole changes the vacuum level across the surface²⁷ as illustrated schematically in Figure 2B. A net increase in the induced surface dipole decreases the work function and increases the magnitude of ΔE_{HOMO} . That the correlation between Φ and ΔE_{HOMO} is not exact can be attributed to the fact that the magnitude of the charge transfer, which also depends on hybridization and steric effects, changes slightly as θ is changed.²⁸

To explore how solvent affects conductance, we need to determine BDA–Au level alignment when a solvent binds to the Au surface, as well as the probability that the solvent binds, which depends on its binding energy. Both factors are important as our calculations, detailed below, show that at fixed coverage, solvent-induced shifts of the work function for our three example solvents are quite similar; however, computed solvent binding energies suggest that their local coverage and induced dipoles are significantly different on Au, leading to changes in work function that explain measured trends in conductance.

To determine BDA–Au level alignment, we add an adsorbate, either another BDA molecule or a solvent molecule, to the other available binding site (Figure 3A) in our 4×4 supercell as illustrated in panels C and D of Figure 3 and compute PDOS on the BDA N. The ClPh, BrPh, or IPh solvent molecules are computed to bind to Au only through the halogen atom within GGA. Example geometries are shown in Figure 3B–D, and corresponding PDOS on the BDA N atom are plotted in Figure 3E. We see that ΔE_{HOMO} is largest when two BDA molecules are bound on the surface in each unit cell since the induced surface dipole is largest in this case. When a BDA is replaced with a solvent molecule, the induced dipole is reduced, and Φ increases up to the limit of one BDA per unit cell. Thus replacing one of the two BDA molecules with a solvent molecule reduces ΔE_{HOMO} .

Noting that the ΔE_{HOMO} is similar for these three solvents, we turn to calculations of the binding energy and thermally averaged

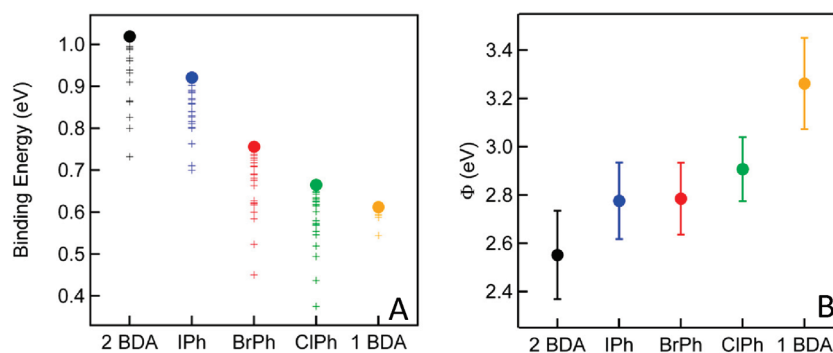


Figure 4. (A) Total binding energy for each system for all structures considered: ●, the maximum computed binding energy; +, the binding energies for all other structures. (B) Thermally averaged work function (Φ) for the five systems considered, averaging between 15 and 25 different structures with different Au–N and Au–halogen binding angles. Error bars represent the standard deviation of all Φ determined for each system relative to the thermally averaged value.

work functions at room temperature. Figure 4A shows the calculated binding energies for a range of geometries where both the BDA and solvent binding angles are varied between 0° and 60° .²⁹ Since ClPh, BrPh, and IPh all have similar molecular structures and polarizabilities, we do not expect inclusion of van der Waals interactions, which are not captured by DFT within the GGA used here, to significantly alter their *relative* binding energies (see Supporting Information). The calculated binding energies per unit cell are largest when both binding sites in the supercell are occupied by BDA molecules and decreases as one BDA is first replaced with a solvent and then removed entirely. Using these binding energies, we calculated a thermally averaged work function of the system (Figure 4B). We see that the thermally averaged Φ increases upon replacement of BDA with a solvent molecule.

We can relate these calculations to the experimental data in the following way: During conductance measurements in a solvent environment, there are undercoordinated Au sites on the tip and surface away from the junction available to both solvent and BDA molecules for binding, in addition to the BDA bridging the junction. For a solvent to bind to (or occupy) a given undercoordinated Au site, its binding energy to Au must be comparable to that of BDA. Our results suggest that the relative coverage of these sites can alter Φ , changing the most probable junction conductance and peak positions in the conductance histograms. Interestingly, this implies that the conductance of two BDA molecules in a junction is not necessarily twice the conductance of a single BDA in a junction.^{30,31}

The energetics computed here imply that, thermodynamically, the system prefers BDA to occupy all uncoordinated surface sites on the tip and substrate during break-junction measurements. However, solvent molecules vastly outnumber the solute ($\sim 10000:1$ for the 1 mM solutions used here). Using the maximum computed binding energy of these systems to approximate the energy barrier to replace a surface-bound BDA with a solvent molecule, we find that the replacement probability is $P_{\text{ClPh}} = 0.01$, $P_{\text{BrPh}} = 0.27$, and $P_{\text{IPh}} = 0.99$ using a simple two-state Boltzmann model for each of the three solvents. ClPh's weak binding energies result in a low replacement probability which points to the general inability of chlorinated solvents to replace BDA around the junction. This result explains why G_{BDA} in ClPh and the other chlorinated solvents measured here is nearly the same (Figure 1B). It also validates the neglect of solvent in several previous theoretical works, since the comparisons were to experiments conducted in a chlorinated solvent.^{11,23} For BDA

dissolved in BrPh, the binding probability for the solvent is significant. This suggests that a wide range of surface environments (and thus work functions) would be sampled over the course of many measurements, thereby leading to both a higher and wider peak as seen in Figure 1A, in contrast to the lower, narrower peak observed for BDA in ClPh. Finally, the high BDA replacement probability of IPh suggests that the probability of BDA junctions forming in this solvent is low. This is in excellent agreement with the experiment, where the conductance histogram peak for BDA + IPh is very small (Figure 1A) and yet at a higher peak value than the others.

In conclusion, we demonstrate that the measured conductance of BDA–Au junctions can be modulated by the solvent environment. First principles calculations explain experiments by showing that the junction work function is altered when solvent molecules bind to undercoordinated Au atoms around the junction. The computed binding probabilities depend on both the energetics and the relative concentration of solvents to BDA. This novel mechanism for modulating molecular junction conductance is suggestive of the rich variety of effects that the environment may have on molecular-scale charge transport properties.

■ ASSOCIATED CONTENT

Supporting Information. Additional data and controls, solvent–BDA interactions, statistical model details, and van der Waals interactions. This material is available free of charge via the Internet at <http://pubs.acs.org>.

■ AUTHOR INFORMATION

Corresponding Author

*E-mail: jbneaton@lbl.gov; lv2117@columbia.edu.

Present Addresses

⁵77 Massachusetts Ave., Bldg. 13-2025, Cambridge, MA 02139.

■ ACKNOWLEDGMENT

We thank M. L. Steigerwald, L. Kronik, I. Tamblin, S. Y. Quek, and A. Zayak for discussions. This work was supported in part by the NSF Career Award (CHE-07-44185) and the ACS PRF. Part of this research was performed at the Molecular Foundry at LBNL, supported by the DOE, Office of Basic Energy Sciences.

V.F. thanks the NSEC REU program at Columbia University and the Science Undergraduate Laboratory Internship Program at LBNL.

REFERENCES

- (1) Joachim, C.; Ratner, M. A. *Proc. Natl. Acad. Sci. U.S.A.* **2005**, *102* (25), 8801–8808.
- (2) Lortscher, E.; Cizek, J. W.; Tour, J.; Riel, H. *Small* **2006**, *2* (8–9), 973–977.
- (3) Nitzan, A.; Ratner, M. A. *Science* **2003**, *300* (5624), 1384–1389.
- (4) Venkataraman, L.; Klare, J. E.; Tam, I. W.; Nuckolls, C.; Hybertsen, M. S.; Steigerwald, M. L. *Nano Lett.* **2006**, *6* (3), 458–462.
- (5) Li, X. L.; He, J.; Hihath, J.; Xu, B. Q.; Lindsay, S. M.; Tao, N. J. *J. Am. Chem. Soc.* **2006**, *128* (6), 2135–2141.
- (6) Li, C.; Pobelov, I.; Wandlowski, T.; Bagrets, A.; Arnold, A.; Evers, F. *J. Am. Chem. Soc.* **2008**, *130* (1), 318–326.
- (7) Wu, S. M.; Gonzalez, M. T.; Huber, R.; Grunder, S.; Mayor, M.; Schonenberger, C.; Calame, M. *Nat. Nanotechnol.* **2008**, *3* (9), 569–574.
- (8) Mishchenko, A.; Vonlanthen, D.; Meded, V.; Burkle, M.; Li, C.; Pobelov, I. V.; Bagrets, A.; Viljas, J. K.; Pauly, F.; Evers, F.; Mayor, M.; Wandlowski, T. *Nano Lett.* **2010**, *10* (1), 156–163.
- (9) Kamenetska, M.; Quek, S. Y.; Whalley, A. C.; Steigerwald, M. L.; Choi, H. J.; Louie, S. G.; Nuckolls, C.; Hybertsen, M. S.; Neaton, J. B.; Venkataraman, L. *J. Am. Chem. Soc.* **2010**, *132* (19), 6817–6821.
- (10) Leary, E.; Hobenreich, H.; Higgins, S. J.; van Zalinge, H.; Haiss, W.; Nichols, R. J.; Finch, C. M.; Grace, I.; Lambert, C. J.; McGrath, R.; Smerdon, J. *Phys. Rev. Lett.* **2009**, *102* (8), 086801.
- (11) Quek, S. Y.; Venkataraman, L.; Choi, H. J.; Louie, S. G.; Hybertsen, M. S.; Neaton, J. B. *Nano Lett.* **2007**, *7* (11), 3477–3482.
- (12) Kiguchi, M.; Miura, S.; Takahashi, T.; Hara, K.; Sawamura, M.; Murakoshi, K. *J. Phys. Chem. C* **2008**, *112* (35), 13349–13352.
- (13) Xu, B. Q.; Tao, N. J. *J. Science* **2003**, *301* (5637), 1221–1223.
- (14) Venkataraman, L.; Klare, J. E.; Nuckolls, C.; Hybertsen, M. S.; Steigerwald, M. L. *Nature* **2006**, *442* (7105), 904–907.
- (15) The list of solvents used is as follows: 1, chlorobenzene; 2, 1,2,4-trichlorobenzene; 3, 1,2-dichlorobenzene; 4, 1-chloronaphthalene; 5, ethyl benzoate; 6, 1,3-dibromobenzene; 7, dimethyl sulfoxide; 8, bromobenzene; 9, tetra(ethylene glycol) dimethyl ether; 10, 1,2-dibromobenzene; 11, 1-bromonaphthalene; 12, iodobenzene; 13, 4-bromoanisole.
- (16) Kresse, G.; Hafner, J. *Phys. Rev. B* **1993**, *47* (1), 558–561.
- (17) Perdew, J. P.; Burke, K.; Ernzerhof, M. *Phys. Rev. Lett.* **1996**, *77* (18), 3865–3868.
- (18) Kresse, G.; Joubert, D. *Phys. Rev. B* **1999**, *59* (3), 1758–1775.
- (19) Neugebauer, J.; Scheffler, M. *Phys. Rev. B* **1992**, *46* (24), 16067–16080.
- (20) Makov, G.; Payne, M. C. *Phys. Rev. B* **1995**, *51* (7), 4014–4022.
- (21) The PDOS of the entire surface-bound molecule has non-HOMO features near the HOMO; by considering only the N nearest to Au, we remove contributions to the DOS from molecular orbitals in this energy range that do not add to the transmission.
- (22) Neaton, J. B.; Hybertsen, M. S.; Louie, S. G. *Phys. Rev. Lett.* **2006**, *97* (21), 216405.
- (23) Quek, S. Y.; Choi, H. J.; Louie, S. G.; Neaton, J. B. *Nano Lett.* **2009**, *9* (11), 3949–3953.
- (24) Dell'Angela, M.; Kladnik, G.; Cossaro, A.; Verdini, A.; Kamenetska, M.; Tamblin, I.; Quek, S. Y.; Neaton, J. B.; Cvetko, D.; Morgante, A.; Venkataraman, L. *Nano Lett.* **2010**, *10* (7), 2470–2474.
- (25) Track, A. M.; Rissner, F.; Heimel, G.; Romaner, L.; Kafer, D.; Bashir, A.; Rangger, G. M.; Hofmann, O. T.; Bucko, T.; Witte, G.; Zojer, E. *J. Phys. Chem. C* **2010**, *114* (6), 2677–2684.
- (26) Magid, I.; Burstein, L.; Seitz, O.; Segev, L.; Kronik, L.; Rosenwaks, Y. *J. Phys. Chem. C* **2008**, *112* (18), 7145–7150.
- (27) Kahn, A.; Koch, N.; Gao, W. Y. *J. Polym. Sci., Part B: Polym. Phys.* **2003**, *41* (21), 2529–2548.
- (28) We see that the width of the N-projected HOMO DOS (not shown) increases (decreases) slightly with increasing (decreasing) bond angle, which increases (decreases) the amount of charge transfer in the bond.
- (29) All binding energies are computed per unit cell. The N–Au bond lengths change by less than 1% among the two-molecule systems studied, indicating that the BDA binding energy is not affected significantly by solvent replacing a BDA.
- (30) Selzer, Y.; Cai, L. T.; Cabassi, M. A.; Yao, Y. X.; Tour, J. M.; Mayer, T. S.; Allara, D. L. *Nano Lett.* **2005**, *5* (1), 61–65.
- (31) Wang, J. G.; Prodan, E.; Car, R.; Selloni, A. *Phys. Rev. B* **2008**, *77* (24), 245443.